Inorganica Chimica Acta, 172 (1990) 211–220

The Synthesis, Molecular Structure and Magnetic Properties of $[Cu_2L(\mu\text{-}OH)CH_3CN]_2[Cu_6I_{10}]$ and $[Cu_2L(\mu\text{-}Br)]Br_2$, where L = 2,6-Bis(*N*,*N*'-dimethylethylenamineformimidoyl)-4-methylphenolato

DALE A. FIRMIN, ESTELLE R. QUILANO, ROBERT CAMERON, ARUN K. PANT*, EDWIN D. STEVENS,
CHARLES J. O'CONNOR**

Department of Chemistry, University of New Orleans, New Orleans, LA 70148 (U.S.A.)

OLIVIER KAHN and TALAL MALLAH

Laboratoire de Chimie Inorganique, URA #420, Université de Paris-Sud, 91405 Orsay (France)

(Received December 21, 1989)

Abstract

The properties of two binuclear copper(II) complexes prepared from the same binucleating ligand are reported. The binuclear units are structurally very similar, but one binuclear unit incorporates a bromine ion into a bridging position, while the other binuclear unit incorporates a hydroxide into the bridge. The intramolecular coupling parameters are $2J = -157$ cm^{-1} and $2J = -478$ cm^{-1} for the bromide and hydroxide bridging analogs, respectively. The hydroxide analog has the unusual feature of a $[Cu_6I_{10}]^{4-}$ hetero-polyanion. Crystal data: complex **A**, $[Cu_2(C_{17}H_{27}N_4O)(OH)(CH_3CN)]_2[Cu_6I_{10}]$, $a = 10.476(3)$, $b = 11.846(6)$, $c = 13.558(7)$ Å, $\alpha = 97.77(4)$, $\beta = 99.62(3)$, $\gamma = 96.33(3)°$, space group $P\bar{1}$, $Z = 2$; complex **B**, $[C_{17}H_{27}N_4O)(Br)]Br_2$, $a = 11.836(2)$, $b = 16.543(4)$, $c = 23.021(5)$ Å, space group *Pbca*, $Z = 8$.

Introduction

We have recently published several reports of binuclear copper(II) complexes that have dissimilar bridging pathways [2–9]. The complexes have the general structure as shown in **1**. The bridging pathways consist of an endogenous phenoxide bridge contained in the binucleating ligand, and a smaller exogeneous bridging ligand (Y). In our previous reports we have prepared a variety of complexes with $Y = Cl^-$ [1], Br^- [2], OH^- [3–5], 1,1-N_3^- [4–6], 1,1-OCN^- [4–6] and 1,3-N_3^- [7].

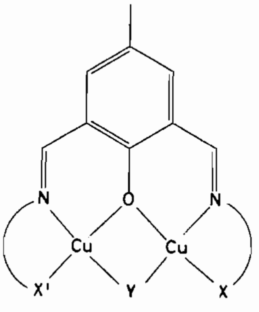

1

There has recently been interest in copper binuclear compounds as chemical models which emulate blue copper proteins [8–12]. Cu(II) complexes analogous to **1**, but with lysine, glutamic acid and arginine side arms (N X), have been shown to have catecholase activity [13, 14]. There have been recent reports of reversible molecular oxygen binding in dinuclear copper complex systems [15, 16]. These types of binuclear copper complexes are potential models for oxyhemocyanin.

The complexes that we have been preparing allow the incorporation of various small molecules into the bridging cavity. Our interest in these complexes arises from the unique ability to make subtle changes in the super exchange pathway by varying the exogenous bridging ligand (Y). We report here on the synthesis, crystal structure and magnetic properties of two new binuclear copper(II) complexes: $[Cu_2L(\mu\text{-}Br)]Br_2$ and $[Cu_2L(\mu\text{-}OH)(CH_3CN)]_2[Cu_6I_{10}]$. The two complexes exhibit normal intra-binuclear antiferromagnetic coupling with singlet triplet splittings of $2J = -478$ cm^{-1} and $2J = -157$ cm^{-1} for the hydroxide and bromide bridged complexes, respectively.

---

*Permanent address: Physics Department, University of Gorakhpur, India.

**Author to whom correspondence should be addressed.

0020-1693/90/$3.50

Experimental

Synthesis

2-Formyl-4-methylsalicylaldimine (Fsal)

Fsal was prepared by the method of Ullman and Brittner [17].

$[Cu_2L(\mu\text{-}OH)(CH_3CN)]_2[Cu_6I_{10}]$ *(A)*

One half mmol Fsal was dissolved in 5 ml 95% EtOH. To this was added 1 mmol DMEN, and 1 mmol of $Cu(BF_4)_2$ dissolved in a small amount of CH_3CN. Next, 2 mmol KI dissolved in a few drops of H_2O were added. After a few days, two types of crystals appeared. One was needle-shaped and slightly soluble in CH_3CN. The other was polygonal and soluble in CH_3CN. The needle-like crystals were separated by washing away the co-precipitate with CH_3CN and drying. The other crystals were recovered by allowing the wash solution to stand and have not yet been characterized.

$[Cu_2L(\mu\text{-}Br)]Br_2$ *(B)*

A 0.200 g sample of Fsal and a 0.545 g sample of copper(II) bromide were dissolved in 50 ml of methanol heated to 70 °C. To this solution, 0.215 g of dimethylethylenediamine was slowly added while stirring. The blue–green liquid turned to aqua upon addition of the dimethylethylenediamine. The solution was stirred for 20 min, forming lime colored microcrystals. The filtered solution was then allowed to evaporate for a few days to 20 ml. The dark olive colored crystals were filtered, washed in methanol, air dried and then dissolved in a solution containing 20 ml of acetonitrile and 30 ml of methanol. The resulting solution was slowly evaporated to about 3 ml. The dark green needle-shaped crystals were then filtered, washed in absolute ethanol and air dried.

Magnetism

The magnetic susceptibilities of the complexes were measured over the 6–350 K temperature region with a superconducting SQUID susceptometer. Measurement and calibration procedures are reported elsewhere [18]. See also 'Supplementary Material'.

Crystallography

Collection and reduction of intensity data

For each of the compounds, single crystal samples were mounted on an Enraf-Nonius CAD-4 four-circle diffractometer. The samples were cooled to 115(2) K using a stream of cold nitrogen gas generated with a locally modified Enraf-Nonius low temperature device. Cell dimensions were determined by least-squares refinement of the measured setting angles of 25 reflections in the range $20° < \theta < 30°$. Space groups were determined by searching for systematically absent reflections, and later confirmed by successful solution of the structure.

Integrated intensity measurements were collected using Mo Kα radiation, a graphite-crystal monochromator, and a θ:2θ scan mode. Scan widths were determined from the formula $SW = A + B \tan\theta$, where the second term accounts for the $K\alpha_1 - K\alpha_2$ splitting. The calculated scan extended at each side by $SW/4$ for background measurements ($BG1$ and $BG2$). The net integrated intensity of each peak was then calculated as $I_{NC} = I_{2/3} - 2(BG1 + BG2)$, where $I_{2/3}$ is the integrated intensity of the central two-thirds portion of the scan. During data collection, three standard reflections were monitored every two hours for changes in intensity, and three high-angle reflections were re-centered after every 200 reflections measured to check for changes in crystal orientation. Decay corrections were calculated from linear least-squares fits to the intensities of the standard reflections. Empirical absorption corrections were applied based on observations of the intensities of three reflections as a function of rotation ψ about the scattering vector. The data were corrected for Lorentz and polarization effects.

Crystal data, intensity measurement conditions and data reduction results are summarized for both compounds in Table 1.

Solution and refinement of structures

The structures of both complexes were solved by direct methods using the program MULTAN80 [19]. The Cu and halogen atom positions were located in the initial E maps, and successive difference Fourier syntheses alternated with full-matrix least-squares refinements revealed the positions of all non-hydrogen atoms. The function $S = \Sigma w(F_o - F_c)^2$ was minimized where $w = 1/(\sigma(F_o))^2$. Standard deviations were estimated by $\sigma(F_o^2) = (\sigma)_{cs}^2 + (0.04F^2)^2)^{1/2}$ where σ_{cs} represents the contribution from counting statistics. Hydrogen atom positions were calculated and included with fixed positions and isotropic thermal parameters. Anisotropic thermal parameters were refined for the Cu and halogen atoms. All other atoms were refined isotropically. Attempts to refine the C, N and O atoms with anisotropic thermal parameters resulted in unrealistic thermal ellipsoids for compound **A**. This may be attributed to errors in the absorption corrections, which could not be reliably calculated because of the irregular shape of the crystal. These errors are also likely to be responsible for the relatively high final R factors. The small size and lack of scattering at high angles from crystals of compound **B** resulted in a large fraction of 'unobserved' reflections, limiting the number of atoms which could be refined anisotropically. All significant peaks in the final difference Fourier maps were located within 0.6 Å of the Cu or halogen atom positions. Comparison of the magnitudes of F_o and

TABLE 1. Crystallographic experimental details

Compound	A	B
a (Å)	10.475(3)	11.836(2)
b (Å)	11.846(6)	16.543(4)
c (Å)	13.558(7)	23.021(5)
α (°)	97.77(4)	90.0
β (°)	99.62(3)	90.0
γ (°)	96.33(3)	90.0
V (Å^3)	1628.2	4507.1
Crystal system	triclinic	orthorhombic
Space group	$P\bar{1}$	*Pbca*
D_{calc} (g/cm^3)	2.680	1.975
Z	2	8
Temperature (K)	115(2)	115(2)
Empirical formula	$Cu_5I_5O_2N_5C_{19}H_{31}$	$Cu_2Br_3O_1N_4C_{17}H_{27}$
Molecular weight	1313.7	670.2
Wavelength $K\alpha_1$ (Å)	0.70930	0.70930
Wavelength $K\alpha_2$ (Å)	0.71359	0.71359
Crystal color, habit	black, irregular needle	dark green, needle
Crystal size (mm)	0.5 × 0.5 × 0.7	0.3 × 0.1 × 0.1
μ (cm^{-1})	79.4	71.8
Crystal decay (%)	3.4	5.1
Range, transmission	0.743 to 0.996	0.926 to 0.995
Limits, 2θ (°)	4 to 50	4 to 40
Limits, h	−11 to 11	0 to 11
Limits, k	−12 to 12	0 to 14
Limits, l	0 to 14	0 to 22
Scan width, A (°)	1.1	1.0
Scan width, B (°)	0.35	0.35
No. reflections	3241	2091
No. reflections with $I > 3r(I)$	3081	1081
No. parameters	171	134
R	0.078	0.044
R_w	0.089	0.048
GOF	11.41	1.34
Max. shift/e.s.d.	0.03	0.01
Max. residual (e/Å^3)	2.29	0.66
Min. residual (e/Å^3)	−2.17	−0.48

F_c for the largest structure factors showed no indication of secondary extinction, and no correction was applied.

Atomic scattering factors and anomalous dispersion corrections were taken from the International Tables for X-ray Crystallography [20]. All computer programs used were from the SDP system [21].

Results and Discussion

Structure

The final positional parameters for the binuclear Cu(II) complexes **A** and **B** are listed in Table 2. Bond distances and angles are given in Tables 3 and 4, respectively. Figures 1(a)–(c) and 2 show perspective views of the molecules together with the numbering schemes.

The main ligand, Fsal, in these complexes is pentadentate and capable of binding two transition metal ions in close proximity. A sixth in-plane bridging coordination site, and the possibility of axial or bridging ligands above and below the plane, generates a large number of possible coordination geometries. Except for the dimethylaminoethane side chains, the Fsal ligand is highly planar in both complexes. The bond lengths and angles within the ligand are very similar in both complexes and comparable to those observed in binuclear Cu(II) complexes of 2,6-bis(*N*-2-pyridylformidolyl)-4-methylphenol [2, 22], a similar ligand.

In complex **A**, an OH^- ion occupies the bridging position. Each Cu atom is five coordinate with a square-pyramidal coordination geometry. The axial coordination site of Cu2 is occupied by a CH_3CN solvent molecule, while the axial coordination site of Cu1 is occupied by I5 of a $[Cu_6I_{10}]^{4-}$ ion which sits

TABLE 2. Positional parameters and their e.s.d.s in parentheses

Atom	x	y	z	B(Å^2)[a]
Complex A				
I1	0.3164(2)	0.0591(2)	0.5547(2)	1.10(5)
I2	−0.0100(2)	0.2370(2)	0.4290(2)	1.19(5)
I3	−0.0238(2)	0.1204(2)	0.7112(2)	1.30(5)
I4	0.2955(2)	−0.0405(2)	0.8320(2)	1.41(5)
I5	0.3418(2)	0.3503(2)	0.8199(2)	1.06(5)
Cu1	0.6412(4)	0.3943(3)	0.8320(3)	0.93(8)
Cu2	0.7088(4)	0.6384(3)	0.8069(3)	0.91(8)
Cu3	0.2453(5)	0.1439(4)	0.7525(5)	3.0(1)
Cu4	0.0931(4)	0.1241(4)	0.5606(4)	1.8(1)
Cu5	0.1420(6)	−0.0502(4)	0.6585(5)	3.3(1)
O1	0.679(2)	0.547(2)	0.907(2)	1.5(5)*
O2	0.646(2)	0.486(2)	0.723(2)	0.7(4)*
N1	0.697(3)	0.710(2)	0.688(2)	0.9(5)*
N2	0.632(3)	0.254(2)	0.741(2)	0.6(5)*
N3	0.687(3)	0.299(2)	0.942(2)	0.7(5)*
N4	0.759(3)	0.797(2)	0.885(2)	1.0(5)*
N5	0.935(3)	0.594(3)	0.802(3)	2.4(7)*
C1	0.649(3)	0.351(3)	0.306(3)	1.2(6)*
C2	0.647(3)	0.384(3)	0.416(3)	1.0(6)*
C3	0.641(3)	0.310(3)	0.484(3)	0.8(6)*
C4	0.640(3)	0.339(3)	0.586(2)	0.6(6)*
C5	0.649(3)	0.453(3)	0.628(3)	1.2(6)*
C6	0.667(3)	0.537(3)	0.561(3)	0.9(6)*
C7	0.661(3)	0.498(3)	0.459(3)	0.7(6)*
C8	0.683(3)	0.657(3)	0.597(2)	0.5(6)*
C9	0.634(3)	0.250(3)	0.647(3)	0.8(6)*
C10	0.724(3)	0.832(3)	0.714(3)	0.8(6)*
C11	0.803(3)	0.861(3)	0.811(3)	1.1(6)*
C12	0.856(3)	0.806(3)	0.973(2)	0.5(6)*
C13	0.649(3)	0.838(3)	0.914(3)	1.0(6)*
C14	0.633(3)	0.157(3)	0.793(3)	1.1(6)*
C15	0.616(3)	0.184(3)	0.889(3)	1.0(6)*
C16	0.828(3)	0.299(3)	0.959(3)	1.1(6)*
C17	0.650(3)	0.337(3)	1.035(3)	1.3(7)*
C18	0.971(4)	0.536(3)	0.746(3)	1.6(7)*
C19	1.018(4)	0.456(3)	0.666(3)	2.1(8)*
Complex B				
Br1	0.1285(2)	0.2333(1)	0.60197(9)	2.02(4)
Br2	−0.0121(2)	−0.0902(1)	0.71635(8)	1.67(4)
Br3	−0.0915(2)	0.0670(1)	0.59419(9)	1.79(4)
Cu1	−0.0440(2)	0.2146(1)	0.6566(1)	1.49(5)
Cu2	0.0679(2)	0.0355(1)	0.6557(1)	1.37(5)
O	0.0240(9)	0.1297(6)	0.7043(5)	1.4(2)*
N1	−0.146(1)	0.2408(8)	0.7225(6)	1.3(3)*
N2	0.209(1)	0.0325(8)	0.7009(6)	1.1(3)*
N3	−0.141(1)	0.2928(8)	0.6101(7)	2.0(3)*
N4	0.158(1)	−0.0321(8)	0.5961(6)	1.5(3)*
C1	0.033(1)	0.129(1)	0.7610(8)	1.7(4)*
C2	0.124(1)	0.086(1)	0.7899(7)	1.0(4)*
C3	0.128(1)	0.083(1)	0.8494(7)	1.0(4)*

(continued)

TABLE 2. *(continued)*

Atom	x	y	z	$B(\AA^2)$[a]
Complex **B**				
C4	0.053(2)	0.122(1)	0.8852(8)	1.8(4)*
C5	−0.030(1)	0.166(1)	0.8597(8)	1.6(4)*
C6	−0.043(1)	0.1710(9)	0.7987(7)	0.8(4)*
C7	0.058(2)	0.115(1)	0.9509(8)	2.7(5)*
C8	0.213(1)	0.0467(9)	0.7551(8)	1.4(4)*
C9	−0.134(1)	0.221(1)	0.7746(7)	1.7(4)*
C10	0.299(2)	−0.008(1)	0.6705(8)	1.8(4)*
C11	−0.235(2)	0.297(1)	0.7057(8)	2.0(4)*
C12	0.250(2)	−0.068(1)	0.6305(8)	1.8(4)*
C13	−0.254(2)	0.291(1)	0.6409(8)	2.2(4)*
C14	0.088(2)	−0.099(1)	0.5685(9)	3.3(5)*
C15	−0.088(2)	0.374(1)	0.6120(8)	2.5(4)*
C16	0.199(2)	0.023(1)	0.5501(8)	2.3(4)*
C17	−0.161(2)	0.271(1)	0.5482(8)	2.4(4)*

[a] Starred items = atoms refined isotropically.

TABLE 3. Bond distances (Å)[a]

Atom 1	Atom 2	Distance	Atom 1	Atom 2	Distance	Atom 1	Atom 2	Distance
Complex A								
I1	Cu3	2.976(2)	Cu1	O2	1.954(6)	N4	C12	1.424(11)
I1	Cu4	2.552(1)	Cu1	N2	1.913(7)	N4	C13	1.398(12)
I1	Cu5	2.797(2)	Cu1	N3	2.022(7)	N5	C18	1.097(12)
I2	Cu4	2.540(1)	Cu2	O1	1.896(7)	C1	C2	1.488(13)
I2	Cu5	2.507(2)	Cu2	O2	1.988(6)	C2	C3	1.374(13)
I3	Cu3	2.756(2)	Cu2	N1	1.912(8)	C2	C7	1.376(13)
I3	Cu4	2.553(1)	Cu2	N4	1.992(7)	C3	C4	1.376(13)
I3	Cu5	2.899(2)	Cu2	N5	2.490(9)	C4	C5	1.379(13)
I4	Cu3	2.629(1)	O2	C5	1.301(11)	C4	C9	1.428(13)
I4	Cu5	2.598(2)	N1	C8	1.287(11)	C5	C6	1.456(13)
I5	Cu1	3.095(1)	N1	C10	1.424(12)	C6	C7	1.382(13)
I5	Cu3	2.525(1)	N2	C9	1.270(12)	C6	C8	1.420(13)
Cu1	Cu2	2.980(2)	N2	C14	1.424(12)	C10	C11	1.408(13)
Cu3	Cu4	2.780(2)	N3	C15	1.500(11)	C14	C15	1.350(13)
Cu3	Cu5	2.506(2)	N3	C16	1.455(12)	C18	C19	1.522(14)
Cu4	Cu5	2.652(2)	N3	C17	1.401(12)			
Cu1	O1	1.915(7)	N4	C11	1.434(12)			
Complex **B**								
Br1	Cu1	2.418(3)	O	C1	1.31(2)	C2	C3	1.37(2)
Br2	Cu2	2.677(3)	N1	C9	1.25(2)	C2	C8	1.47(2)
Br3	Cu1	2.889(3)	N1	C11	1.45(2)	C3	C4	1.38(2)
Br3	Cu2	2.416(3)	N2	C8	1.27(2)	C4	C5	1.34(2)
Cu1	O	1.956(10)	N2	C10	1.44(2)	C4	C7	1.52(2)
Cu1	N1	1.988(13)	N3	C13	1.51(2)	C5	C6	1.41(2)
Cu1	N3	2.035(14)	N3	C15	1.49(2)	C6	C9	1.46(2)
Cu2	O	1.988(10)	N3	C17	1.49(2)	C10	C12	1.48(2)
Cu2	N2	1.968(13)	N4	C12	1.47(2)	C11	C13	1.51(3)
Cu2	N4	2.066(13)	N4	C14	1.52(2)	C1	C2	1.45(2)
			N4	C16	1.48(2)	C1	C6	1.44(2)

[a] Numbers in parentheses are e.s.d.s in the least significant digits.

TABLE 4. Bond angles (°)

Atom 1	Atom 2	Atom 3	Angle	Atom 1	Atom 2	Atom 3	Angle	Atom 1	Atom 2	Atom 3	Angle
Complex A											
Cu3	I1	Cu4	59.81(4)	I3	Cu4	Cu3	62.05(5)	N1	Cu2	N5	94.3(3)
Cu3	I1	Cu5	51.34(4)	I3	Cu4	Cu5	67.67(5)	N4	Cu2	N5	97.1(3)
Cu4	I1	Cu5	59.24(4)	Cu3	Cu4	Cu5	54.87(5)	C8	N1	C10	123.3(8)
Cu4	I2	Cu5	86.82(5)	I1	Cu5	I2	117.65(7)	C9	N2	C14	124.4(8)
Cu3	I3	Cu4	63.04(5)	I1	Cu5	I3	104.91(5)	C15	N3	C16	111.2(7)
Cu3	I3	Cu5	52.53(4)	I1	Cu5	I4	99.55(5)	C15	N3	C17	114.9(7)
Cu4	I3	Cu5	57.80(4)	I1	Cu5	Cu3	68.01(6)	C16	N3	C17	108.8(7)
Cu3	I4	Cu5	57.29(4)	I1	Cu5	Cu4	55.77(4)	C11	N4	C12	112.1(7)
Cu1	I5	Cu3	113.08(5)	I2	Cu5	I3	111.59(6)	C11	N4	C13	110.0(7)
I5	Cu1	Cu2	107.33(4)	I2	Cu5	I4	120.19(6)	C12	N4	C13	107.5(7)
I1	Cu3	I3	103.95(5)	I2	Cu5	Cu3	172.15(9)	C1	C2	C3	125.4(8)
I1	Cu3	I4	94.48(5)	I2	Cu5	Cu4	112.73(6)	C1	C2	C7	121.4(9)
I1	Cu3	I5	112.65(6)	I3	Cu5	I4	100.55(6)	C3	C2	C7	113.1(8)
I1	Cu3	Cu4	52.51(4)	I3	Cu5	Cu3	60.79(5)	C2	C3	C4	126.4(8)
I1	Cu3	Cu5	60.65(6)	I3	Cu5	Cu4	54.53(4)	C3	C4	C5	119.7(9)
I3	Cu3	I4	103.63(5)	I4	Cu5	Cu3	61.96(5)	C3	C4	C9	119.3(8)
I3	Cu3	I5	111.11(6)	I4	Cu5	Cu4	126.98(6)	C5	C4	C9	121.0(8)
I3	Cu3	Cu4	54.91(4)	Cu3	Cu5	Cu4	65.16(5)	O2	C5	C4	122.8(9)
I3	Cu3	Cu5	66.68(5)	O1	Cu1	O2	79.2(3)	O2	C5	C6	120.4(8)
I4	Cu3	I5	127.83(6)	O1	Cu1	N2	167.3(3)	C4	C5	C6	116.8(8)
I4	Cu3	Cu4	120.58(6)	O1	Cu1	N3	101.4(3)	C5	C6	C7	118.3(8)
I4	Cu3	Cu5	60.75(5)	O2	Cu1	N2	91.8(3)	C5	C6	C8	121.4(8)
I5	Cu3	Cu4	111.16(6)	O2	Cu1	N3	164.9(3)	C7	C6	C8	120.3(8)
I5	Cu3	Cu5	170.79(8)	N2	Cu1	N3	84.9(3)	C2	C7	C6	125.5(9)
Cu4	Cu3	Cu5	59.97(5)	O1	Cu2	O2	78.8(3)	N1	C8	C6	129.9(8)
I1	Cu4	I2	120.96(5)	O1	Cu2	N1	165.4(3)	N2	C9	C4	131.3(9)
I1	Cu4	I3	124.47(6)	O1	Cu2	N4	103.7(3)	N1	C10	C11	109.1(8)
I1	Cu4	Cu3	67.68(5)	O1	Cu2	N5	95.3(3)	N4	C11	C10	113.7(8)
I1	Cu4	Cu5	64.98(5)	O2	Cu2	N1	90.7(3)	N2	C14	C15	112.0(8)
I2	Cu4	I3	113.46(5)	O2	Cu2	N4	174.9(3)	N3	C15	C14	114.2(8)
I2	Cu4	Cu3	144.14(6)	O2	Cu2	N5	87.1(3)	N5	C18	C19	178(1)
I2	Cu4	Cu5	160.41(7)	N1	Cu2	N4	86.0(3)	Cu2	N5	C18	130.1(8)
Complex B											
Br1	Cu1	Br3	90.77(9)	N4	C12	C10	111(1)				
Br1	Cu1	O	92.1(3)	N3	C13	C11	110(2)				
Br1	Cu1	N1	152.0(4)	C9	N1	C11	120(2)				
Br1	Cu1	N3	97.0(4)	C8	N2	C10	122(1)				
Br3	Cu1	O	75.6(3)	C13	N3	C15	112(1)				
Br3	Cu1	N1	116.4(4)	C13	N3	C17	108(1)				
Br3	Cu1	N3	99.5(4)	C15	N3	C17	108(1)				
O	Cu1	N1	88.8(5)	C12	N4	C14	109(1)				
O	Cu1	N3	169.8(5)	C12	N4	C16	113(1)				
N1	Cu1	N3	85.4(6)	C14	N4	C16	109(1)				
Br2	Cu2	Br3	101.35(9)	O	C1	C2	122(2)				
Br2	Cu2	O	102.8(3)	O	C1	C6	123(2)				
Br2	Cu2	N2	90.3(4)	C2	C1	C6	115(2)				
Br2	Cu2	N4	96.3(4)	C1	C2	C3	120(2)				
Br3	Cu2	O	87.5(3)	C1	C2	C8	120(2)				
Br3	Cu2	N2	167.9(4)	C3	C2	C8	120(2)				
Br3	Cu2	N4	97.5(4)	C2	C3	C4	124(2)				
O	Cu2	N2	86.8(5)	C3	C4	C5	117(2)				

(continued)

TABLE 4. *(continued)*

Atom 1	Atom 2	Atom 3	Angle	Atom 1	Atom 2	Atom 3	Angle	Atom 1	Atom 2	Atom 3	Angle
Complex **B**											
O	Cu2	N4	158.9(5)	C3	C4	C7	122(2)				
N2	Cu2	N4	84.2(5)	C5	C4	C7	121(2)				
N2	C8	C2	126(2)	C4	C5	C6	123(2)				
N1	C9	C6	127(2)	C1	C6	C5	120(2)				
N2	C10	C12	109(1)	C1	C6	C9	120(2)				
N1	C11	C13	109(2)	C5	C6	C9	120(2)				

Numbers in parentheses are e.s.d.s in the least significant digits.

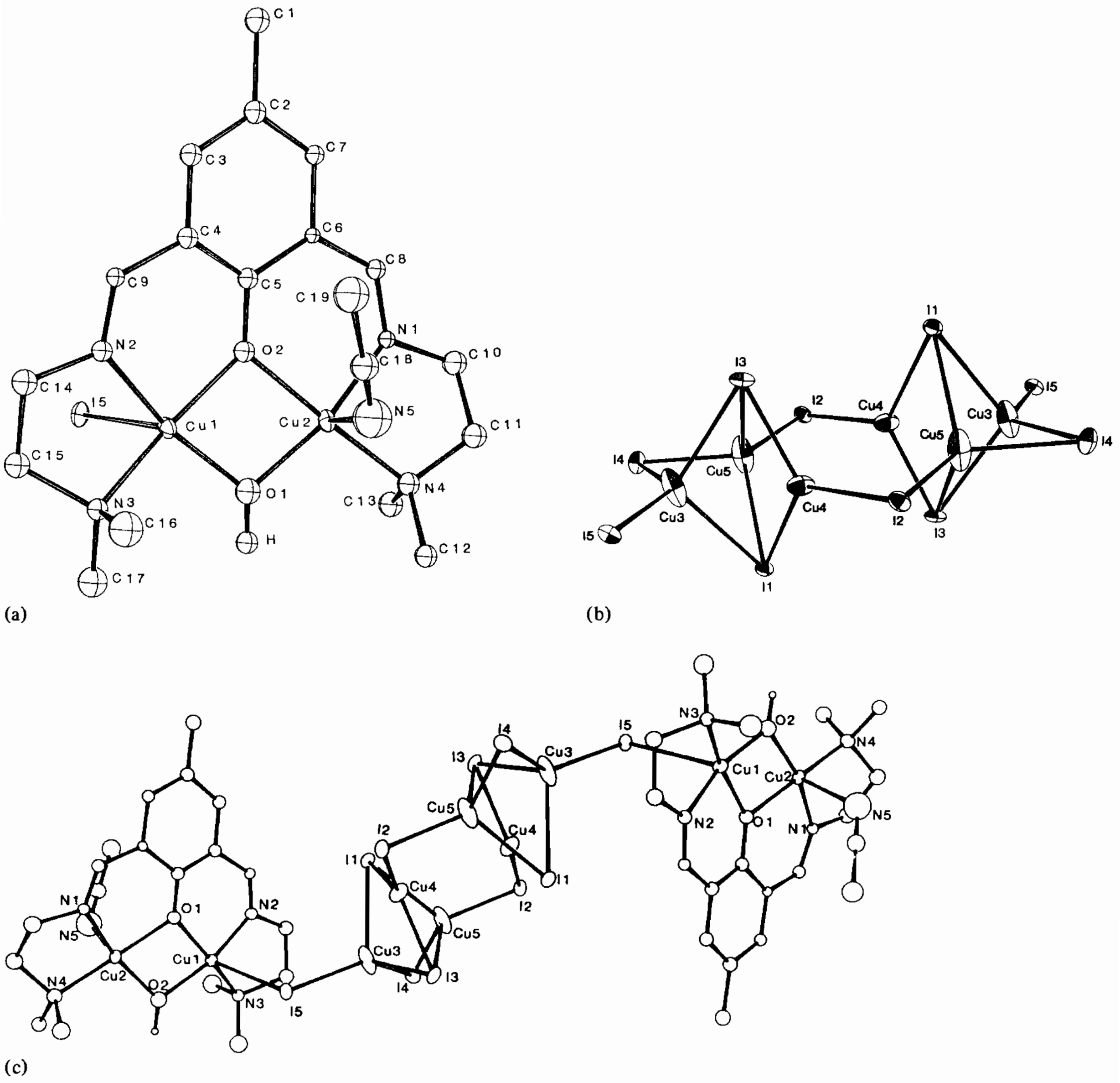

Fig. 1. ORTEP diagrams of: (a) the binuclear $(Cu_2L(\mu\text{-}OH))^{2+}$ unit; (b) the $(Cu_6I_{10})^{4-}$ cluster; (c) the asymmetric unit of the $[Cu_2L(\mu\text{-}OH)]_2(Cu_6I_{10})$ crystalline material.

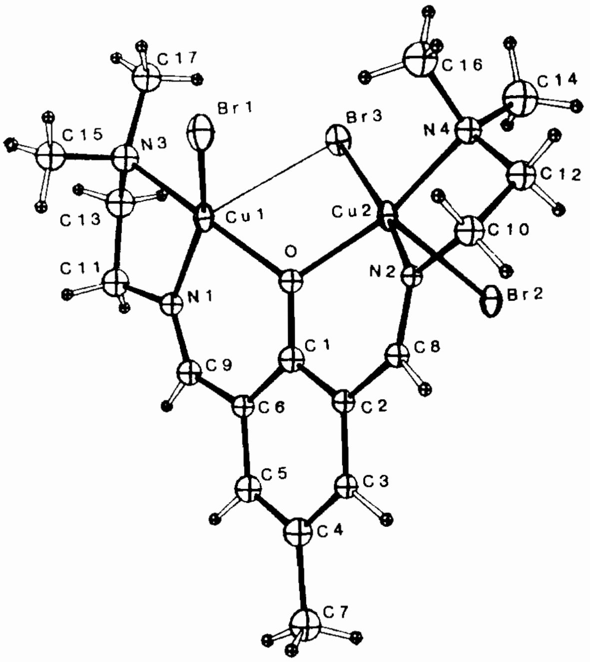

Fig. 2. ORTEP diagram of the binuclear $[Cu_2L(\mu\text{-Br})]^{2+}$ unit of the $[Cu_2L(\mu\text{-Br})]Br_2$ crystalline material.

on a crystallographic inversion center and bridges between two binuclear units. The axial ligands lie on opposite sides of the plane of the Fsal ligand. Cu1 lies 0.213(4) Å above the plane defined by O1, O2, N2 and N3, while Cu2 lies 0.124(4) Å above the plane defined by O1, O2, N1 and N4. The bridging angles between the ligands and the two copper(II) centers are 102.9(3)° for Cu1–O1–Cu2 and 98.2(3)° for Cu1–O2–Cu2.

The $[Cu_6I_{10}]^{4-}$ ion consists of two triangular clusters of Cu(I) atoms which are linked by bridging I atoms (I2 and I4) and capped by two I atoms (I1 and I3). The geometry of I atoms about Cu3 and Cu5 is tetrahedral while the geometry at Cu4 is approximately trigonal. There are several other reports of copper(I) iodide clusters, including $[Cu_2I_4]^{2-}$ [23], $[Cu_2I_6]^{4-}$ [23], $[Cu_3I_4]^{-}$ [24], $[Cu_4I_6]^{2-}$ [25], $[CuI_3]^{2-}$ [26] and $[Cu_{36}I_{56}]^{20-}$ [27].

In complex **B**, a Br^- ion occupies the bridging position. Each Cu atom is again five coordinate with approximate square-pyramidal coordination geometry. Unlike complex A, however, in complex **B**, the bridging ion occupies the axial coordination site of the square pyramid at Cu1. At Cu2, the bridging ligand forms part of the base of the pyramid, as in complex A. This unusual coordination geometry is also reflected in the asymmetry of the bonds to the bridging ligand, with lengths of 2.889(3) and 2.416(3) Å for Cu1–Br3 and Cu2–Br3, respectively. The bridging angles between the oxygen and bromine ligands and the two copper(II) centers are 110.9(3)° for Cu1–O–Cu2 and 74.9(1)° for Cu1–Br3–Cu2. A similar, although smaller, asymmetry is observed in the corresponding complex of 2,6-bis(*N*-2-pyridylformidolyl)-4-methylphenol with Br^- in the bridging and axial positions [2]. Cu1 lies 0.206(2) Å above the least-squares plane through Br1, O, N1 and N3, while Cu2 lies 0.284(2) Å above the plane of Br3, O, N2 and N4.

Magnetism

The magnetic susceptibility data for the complexes is plotted as a function of temperature in Figs. 3 and 4. Each of the data curves exhibits magnetic susceptibility behavior that is consistent with antiferromagnetic coupling between the two copper(II) ions in the binuclear unit; $[Cu_2L(\mu\text{-Br})]Br_2$ has a maximum around 60 K and $[Cu_2L(\mu\text{-OH})(CH_3CN)]_2[Cu_6I_{10}]$ has its maximum above room temperature. The

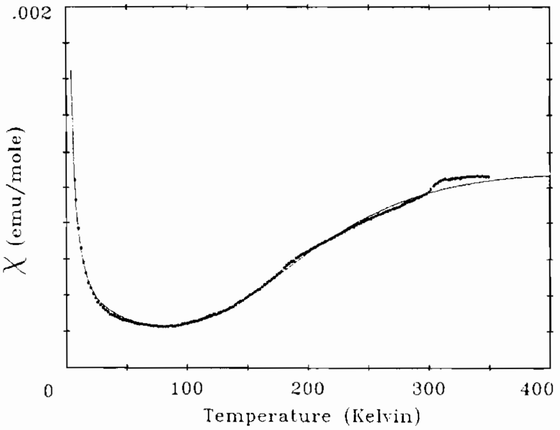

Fig. 3. Plot of the magnetic susceptibility as a function of temperature for $[Cu_2L(\mu\text{-OH})](Cu_6I_{10})_{0.5}$. The smooth curve plotted through the data points is the best fit of eqn. (1) to the data as described in text.

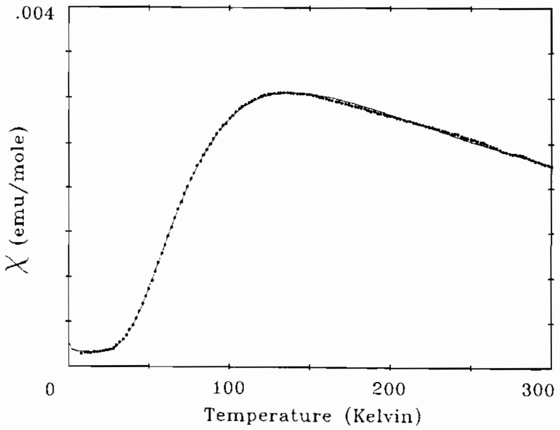

Fig. 4. Plot of the magnetic susceptibility as a function of temperature for $[Cu_2L(\mu\text{-Br})]Br_2$. The smooth curve plotted through the data points is the best fit of eqn. (1) to the data as described in text.

TABLE 5. Fitted magnetic parameters for the two copper(II) binuclears as described in text

Complex	g	J ($\mathrm{cm^{-1}}$)	*TIP* (emu/mol Cu)	Impurity (%)
$[\mathrm{Cu_2L}(\mu\text{-Br})]\mathrm{Br_2}$	2.07	−157	0.000082	
$[\mathrm{Cu_2L}(\mu\text{-OH})(\mathrm{CH_3CN})]_2[\mathrm{Cu_6I_{10}}]$	2.05	−478	0.000075	1.5

iodide complex exhibited signs of decomposition when the specimen was heated above approximately 300 K, and therefore attempts to resolve the maximum expected at higher temperatures were unsuccessful. The decomposition of the sample above 300 K was checked by re-cooling the heated sample back to 6 K. A plot of the magnetic data as a function of temperature for this thermally recycled sample showed pronounced differences in shape and magnitude, and verified the decomposition of the sample at elevated temperatures.

The type of non-Curie–Weiss behavior that is observed in these two compounds is consistent with antiferromagnetic coupling between the two copper(II) ions ($S_1 = S_2 = 1/2$) of the binuclear unit. The equation that describes the temperature dependence of the magnetic susceptibility of a copper(II) binuclear is given in eqn. (1).

$$\chi = \frac{2Ng^2\mu_B{}^2}{kT}\;\frac{\exp^x}{1 - 3\exp^x} \qquad (1)$$

where $x = 2J/kT$, and $2J$ is the singlet triplet splitting with a negative J value denoting a ground state singlet. The data were also corrected for the presence of temperature independent paramagnetism before fitting with this equation. Complex **A** (the hydroxide bridged complex) also required a small correction for the presence of a paramagnetic (monomeric) impurity. Both complexes gave excellent fits of eqn. (1) to the experimental data using the parameters listed in Table 5.

The hydroxide bridged complex exhibits a much larger exchange constant compared to the bromine bridged complex. This is as expected from our previous studies comparing hydroxide and bromide bridges. It is interesting to note that the bromine bridged pathway is longer than might be expected due to the axial type bond of Br3 to Cu1. This distance is close to a non-bonding distance and might be expected to have a negligible contribution to the magnetic exchange when compared to the phenoxide bridge. In the hydroxide bridged complex, on the other hand, both the hydroxide and the phenoxide bridges would be expected to contribute to the overall magnetic exchange.

The results that we have obtained on these materials are consistent with our previous observations of the magnetic properties of binuclear copper(II) molecules with exogenous bridging ligands. The effectiveness of the exogenous ligands may be ordered according to their ability to propagate antiferromagnetic exchange. Since the phenoxide bridge by itself would be expected to propagate a moderate antiferromagnetic exchange component, the smaller values of magnetic coupling constants that we have observed in some of these complexes are likely due to a ferromagnetic exchange influence. The ordering of the ligands from strong antiferromagnetic to weak ferromagnetic coupling is as follows: $1,3\text{-}\mathrm{N_3}^-$, OH^-, Br^-, Cl^-, $\mathrm{CH_3CO_2}^-$, $1,1\text{-}\mathrm{N_3}^-$. All of the data have been recorded on copper(II) binuclear complexes. It is planned to extend this study to binuclear metal complexes other than copper in order to test the efficiency of these ligands for the propagation of magnetic exchange when coupled to metals with higher spin states.

Acknowledgements

C.J.O. wishes to acknowledge support from the Louisiana Education Quality Support Fund administered by the Board of Regents of the state of Louisiana and the donors of the Petroleum Research Fund administered by the Americal Chemical Society.

References

1 E. E. Eduok and C. J. O'Connor, *Inorg. Chim. Acta, 88* (1984) 229.

2 C. J. O'Connor, D. A. Frmin, A. K. Pant, B. Ram Babu and E. D. Stevens, *Inorg. Chem., 25* (1986) 2300.

3 T. N. Sorrell, D. L. Jameson and C. J. O'Connor, *Inorg. Chem., 23* (1984) 190.

4 M. L. Boillot, O. Kahn, C. J. O'Connor, J. Gouteron, S. Jeannin and Y. Jeannin, *J. Chem. Soc., Chem. Commun.,* (1985) 178.

5 T. Mallah, M. L. Boillot, O. Kahn, J. Gouteron, S. Jeannin and Y. Jeannin, *Inorg. Chem., 25* (1986) 3058.

6 T. Mallah, O. Kahn, J. Gouteron, S. Jeannin, Y. Jeannin and C. J. O'Connor, *Inorg. Chem., 26* (1987) 1375.

7 O. Kahn, T. Mallah, J. Gouteron, S. Jeannin and Y. Jeannin, *J. Chem. Soc., Dalton Trans.,* in press.

8 T. N. Sorrell, C. J. O'Connor, O. P. Anderson and J. H. Reibenspies, *J. Am. Chem. Soc., 107* (1985) 4199.

9 V. McKee, M. Zvagulis, J. V. Dadgegian, M. G. Patch and C. A. Reed, *J. Am. Chem. Soc., 106* (1984) 4765.

10 J. Lorosch, W. Haase and P. V. Huong, *J. Inorg. Biochem., 27* (1986) 53.
11 W. P. J. Gaykema, W. G. J. Hol, J. M. Vereijken, N. M. Soeter, H. J. Bak and J. J. Beintema, *Nature (London), 309* (1984) 23.
12 E. I. Solomon, in T. G. Spiro (ed.), *Copper Proteins,* Wiley, New York, 1981, Ch. 1.
13 E. I. Solomon, K. W. Penfield and D. E. Wilcox, *Struct. Bonding (Berlin), 53* (1983) 1.
14 K. Moore and G. S. Vigee, *Inorg. Chim. Acta, 66* (1982) 125.
15 K. D. Karlin, M. S. Haka, R. W. Cruse and Y. Gultnen, *J. Am. Chem. Soc., 107* (1985) 5828.
16 K. D. Karlin, R. W. Cruse, M. S. Haka, Y. Gultnen and B. L. Cohen, *Inorg. Chim. Acta, 125* (1986) L43.
17 F. Ullman and K. Brittner, *Ber. Dtsch. Chem. Ges.,* (1909) 2539.
18 C. J. O'Connor, *Prog. Inorg. Chem., 29* (1982) 203.
19 P. Main, S. J. Fiske, S. E. Hull, L. Lessinger, G. Germaine, J. P. Declercq and M. M. Woolfson, *MULTAN 80,* a system of computer programs for the automatic solution of crystal structures from X-ray diffraction data, Universities of York, U. K. and Louvain, Belgium, 1980.
20 *International Tables for X-ray Crystallography,* Vol. IV, Kynoch, Birmingham, U.K., 1974.
21 B. A. Frenz, in H. Schenk, R. Olthof-Hazekamp, H. van Koningsveld and G. C. Bassi (eds.), *Computing in Crystallography,* Delft University Press, Delft, The Netherlands, 1982.
22 R. J. Majeste, C. L. Klein and E. D. Stevens, *Acta Crystallogr., Sect. C, 39* (1983) 52.
23 H. Hartl, I. Brudgam and F. Mahdjour-Hasson-Abadi, *Z. Naturforsch., Teil B, 40* (1985) 1032.
24 H. Rath and E. M. Holt, *J. Chem. Soc., Chem. Commun.,* (1985) 665.
25 N. P. Rath, E. M. Holt and K. Tonimura, *Inorg. Chem., 24* (1985) 3934.
26 G. A. Bowmaker, G. R. Clark and D. A. Rogers, *J. Chem. Soc., Dalton Trans.,* (1984) 37.
27 H. Hartl and J. Fuchs, *Angew. Chem., Int. Ed. Engl., 25* (1986) 569.